Supplementary Material

Formation of $PPh_2C_6F_5$ through Phosphido Platinum and/or Palladium(III) Intermediates[§]

Irene Ara,[a] Naima Chaouche,[a,b] Juan Forniés,*[a] Consuelo Fortuño[a], Abdelaziz Kribii[b] and Athanassios C. Tsipis*[c]

[a] *Departamento de Química Inorgánica and Instituto de Ciencia de Materiales de Aragón, Universidad de Zaragoza-CSIC , 50009 Zaragoza, Spain.*

[b] *Département de Chimie, Faculté des Sciences, Université IbnTofail, B. P. 133, Kenitra, Morocco*

[c] *Laboratory of Inorganic Chemistry, Department of Chemistry, University of Ioannina, 451 10 Ioannina, Greece*

List of authors in Ref. 64.

(64) Frisch, M. J. T., G. W.; Schlegel, H. B.; Scusseria, G. E.; Robb, M. A.; Cheeseman, J. R.; Zakrzewski, V. G.; Montgomery, J. A.; Vreven, T.; Kudin, K. N.; Burant, J. C.; Millan, J. M.; Iyengar, S. S.; Tomasi, J.; Barone, V.; Mennucci, B.; Cossi, M.; Scalmani, G.; Rega, N.; Petersson, G. A.; Nakatsuji, H.; Hada, M.; Ehara, M.; Toyota, K.; Fukuda. R.; Hasegawa, J.; Ishida, M.; Nakajima, T.; Honda, Y.; Kitao, O.; Nakai, H.; Klene, M.; Li, X.; Knox, J. E.; Hratchian, H. P.; Cross, J. B.; Adamo, C.; Jaramillo, J.; Gomperts, R.; Stratmann, R. E.; Yazyev, O.; Austin, A. J.; Cammi, R.; Pomelli, C.; Ochterski, J. W.; Ayala, P. Y.; Morokuma, K.; Voth, G. A.; Salvador, P.; Dannenberg, J. J.; Zakrzewski, V. G.; Dapprich, S.; Daniels, A. D.; Strain, M. C.; Farkas, O.; Malick, D. K.; Rabuck, A. D.; Raghavachari, K.; Foresman, J. B.; Ortiz, J. V.; Cui, Q.; Baboul, A. G.; Clifford, S.; Cioslowski, J.; Stefanov, B. B.; Liu, G.; Liashenko, A.; Piskorz, P.; Komaromi, I.; Martin, R. L.; Fox, D. J.; Keith, T.; Al-Laham, M. A.; Peng, C. Y.; Nanayakkara, A.; Challacombe, M.; Gill, P. M. W.; Johnson, B.; Chen, W.; Wong, M. W.; Gonzalez, C.; Pople, J. A., Gaussian 03, Revision B 02, Gaussian, Inc.: Pittsburgh PA, 2003.

DFT Calculations of the Geometric and Energetic Profile of the Reaction of $[(C_6F_5)_2M(\mu\text{-}PH_2)_2M'(NCCH_3)_2]$ (M = M' = Pt or Pd, M = Pt, M' = Pd) Complexes with I_2 in the Gas-Phase. To furnish details on the structural and energetic changes that accompany the reaction of the neutral $[(C_6F_5)_2M(\mu\text{-}PH_2)_2M'(NCCH_3)_2]$ (M = M' = Pt or Pd, M = Pt, M' = Pd) complexes with I_2, the potential energy surfaces (PES) of the reactions in the gas-phase were computed by DFT methods (at the B3LYP/lanl2dz level). Because of the computational cost due to the relatively big size of the compounds under consideration, to obtain a computationally convenient size, we used models resulting upon substitution of only the phenyl groups of the phosphido ligands by H atoms. Furthermore, the formation of the neutral $[(C_6F_5)_2M(\mu\text{-}PH_2)_2M'(NCCH_3)_2]$ (M = M' = Pt or Pd, M = Pt, M' = Pd) complexes upon acidifying acetonitrile solutions of $[(C_6F_5)_2Pt(\mu\text{-}PH_2)_2Pd(C_6F_5)_2]^{2-}$ and $[(C_6F_5)_2Pd(\mu\text{-}PH_2)_2Pd(acac)]^-$ complexes has also been investigated at the B3LYP/lanl2dz level of theory.

Equilibrium Geometry, Electronic Structure, and Bonding Mechanism in the Precursor $[(C_6F_5)_2Pt(\mu\text{-}PH_2)_2Pd(C_6F_5)_2]^{2-}$ and $[(C_6F_5)_2Pd(\mu\text{-}PH_2)_2Pd(acac)]^-$ Complexes. Let us first explore the details of the structural, energetic and electronic properties of the precursor $[(C_6F_5)_2Pt(\mu\text{-}PH_2)_2Pd(C_6F_5)_2]^{2-}$ and $[(C_6F_5)_2Pd(\mu\text{-}PH_2)_2Pd(acac)]^-$ complexes. Selected geometrical parameters of the $[(C_6F_5)_2Pt(\mu\text{-}PH_2)_2Pd(C_6F_5)_2]^{2-}$ and $[(C_6F_5)_2Pd(\mu\text{-}PH_2)_2Pd(acac)]^-$ complexes are given in Figure 3S, while their total electronic energies, and some electronic properties are compiled in Table 3S.

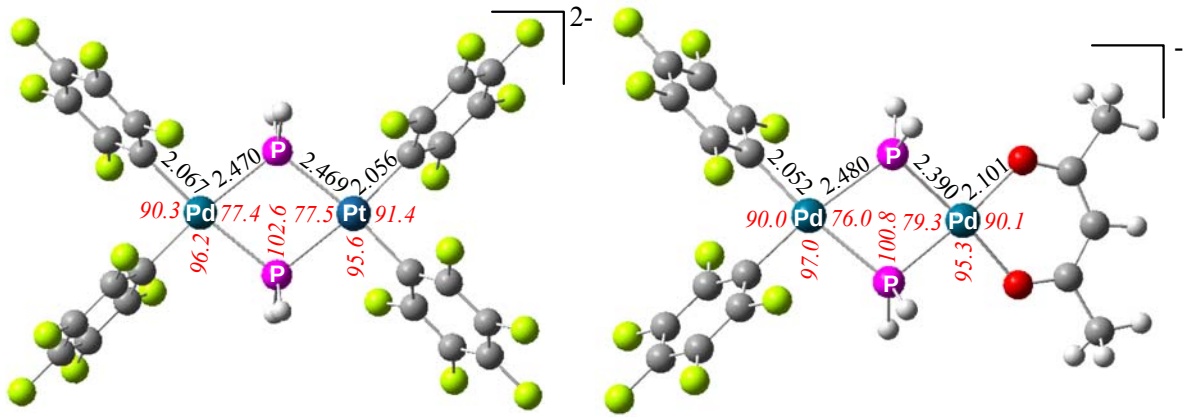

Figure 3S. Equilibrium geometries (bond lengths in Å, bond angles in deg) of the $[(C_6F_5)_2Pt(\mu\text{-}PH_2)_2Pd(C_6F_5)_2]_{2-}$ and $[(C_6F_5)_2Pd(\mu\text{-}PH_2)_2Pd(acac)]$- complexes computed at the B3LYP/lanl2dz level.

Table 3S. Total Electronic Energies and Selected Electronic Properties of the $[(C_6F_5)_2Pt(\mu\text{-}PH_2)_2Pd(C_6F_5)_2]^{2-}$ and $[(C_6F_5)_2Pd(\mu\text{-}PH_2)_2Pd(acac)]^-$ Complexes Computed at the B3LYP/lanl2dz Level of Theory

Property	$[(C_6F_5)_2Pt(\mu\text{-}PH_2)_2Pd(C_6F_5)_2]^{2-}$	Property	$[(C_6F_5)_2Pd(\mu\text{-}PH_2)_2Pd(acac)]^-$
E (hartrees)	-3172.70507	E (hartrees)	-2069.81990
ε_{HOMO} (eV)	-1.43	ε_{HOMO} (eV)	-3.73
ε_{LUMO} (eV)	2.84	ε_{LUMO} (eV)	0.44
η (eV)[a]	2.14	η (eV)	2.09
q_{Pt}[b]	0.53 (0.23)[c]	$q_{Pd(R)}$	0.42 (0.07)
q_{Pd}	0.41 (0.03)	$q_{Pd(acac)}$	0.50 (-0.08)
$q_{C(pt)}$	-0.35 (-0.28)	$q_{C(R)}$	-0.32 (-0.07)
$q_{C(pd)}$	-0.33 (-0.05)	$q_{O(acac)}$	-0.71 (-0.39)
nec(Pt)[d]	$6s^{0.59}5d^{9.06}$	*nec*$(Pd)_R$	$5s^{0.41}4d^{9.16}$
nec(Pd)	$5s^{0.42}4d^{9.76}$	*nec*$(Pd)_{acac}$	$5s^{0.40}4d^{9.08}$

[a] Hardness, $\eta = (\varepsilon_{LUMO} - \varepsilon_{HOMO})/2$. [b] Natural charges. [c] Figures in parentheses are the Mulliken net atomic charges. [d] Natural electron configuration.

Interestingly the most salient structural features of the $[(C_6F_5)_2Pt(\mu\text{-}PPh_2)_2Pd(C_6F_5)_2]^{2-}$ and $[(C_6F_5)_2Pd(\mu\text{-}PPh_2)_2Pd(acac)]^-$ complexes are reproduced well by the B3LYP/lanl2dz calculations. Thus, the core structure of the $[(C_6F_5)_2Pt(\mu\text{-}PH_2)_2Pd(C_6F_5)_2]^{2-}$ and $[(C_6F_5)_2Pd(\mu\text{-}PH_2)_2Pd(acac)]^-$ complexes consists of a $Pt(\mu\text{-}P)_2Pd$ and $Pd(\mu\text{-}P)_2Pd$ "rhombus", respectively with the metal centers being four-coordinated forming a square planar coordination environment. The two edge-sharing square planes are co-planar in the $[(C_6F_5)_2Pt(\mu\text{-}PH_2)_2Pd(C_6F_5)_2]^{2-}$ anion, but are slightly folded in the$[(C_6F_5)_2Pd(\mu\text{-}PH_2)_2Pd(acac)]^-$ complex with a Pd-P-Pd-P dihedral angle of 13.2º, very close to that of 16.0º determined experimentally for the $[(C_6F_5)_2Pt(\mu\text{-}PPh_2)_2Pd(acac)]^-$ analogue.[20] The coordination environment of the Pd central atom involving the coordinated acac ligand closely resembles the corresponding coordination environment in the $[(C_6F_5)_2Pt(\mu\text{-}PPh_2)_2Pd(acac)]^-$ analogue. The computed Pd-O bond lengths of 2.101 Å is almost the same with the Pd-O bond lengths of 2.105 Å determined experimentally for the $[(C_6F_5)_2Pt(\mu\text{-}PPh_2)_2Pd(acac)]^-$ analogue.[20] The same holds also true for the computed O-Pd-O bond angle of 90.1º (the experimental value for the $[(C_6F_5)_2Pt(\mu\text{-}PPh_2)_2Pd(acac)]^-$ analogue is 90.07º).[20] The long intermetallic Pt···Pd and Pd···Pd distances of 3.854 and 3.752 Å, respectively preclude any kind of intermetallic interactions. The absence of intermetallic interactions is also mirrored on the large Pt-P-Pd

and Pd-P-Pd bond angles of 102.6 and 100.8º, respectively. Noteworthy is the excellent agreement between the computed harmonic vibrational frequencies (unscalled) of 1568 and 1500 cm^{-1} due to the ν(C=C) and ν(C=O) vibrational modes of the coordinated acac ligand, respectively and the experimental values of 1582 and 1512 cm^{-1}, observed for the $[(C_6F_5)_2PtPd(\mu\text{-}PPh_2)_2Pd(acac)]^-$ analogue.[20]

Perusal of Table 3S illustrates that the nucleophilic centers in the $[(C_6F_5)_2Pt(\mu\text{-}PH_2)_2Pd(C_6F_5)_2]^{2-}$ and $[(C_6F_5)_2Pd(\mu\text{-}PH_2)_2Pd(acac)]^-$ complexes are the C_{ipso} atoms of the coordinated C_6F_5 ligands and the O donor atoms of the coordinated acac ligand, respectively, for these atoms bear the higher negative natural atomic charges. Therefore, protonation of the complexes taking place on these nucleophilic centers enforces the dissociation of the protonated ligand and the creation of vacant coordination sites for the acetonitrile solvent molecules to occupy. The dissociation process of the C_6F_5 ligand coordinated either to Pt or Pd metal centers in the $[(C_6F_5)_2Pt(\mu\text{-}PH_2)_2Pd(C_6F_5)_2]^{2-}$ dianion promoted by the protonation is predicted to be exothermic with an exothermicity estimated to be about 184 and 192 kcal/mol, respectively at the B3LYP/lanl2dz level. Similarly, the dissociation of the *acac* ligand promoted by protonation is also an exothermic process, the exothermicity estimated to be about 89 kcal/mol at the B3LYP/lanl2dz level. The electrostatically controlled interactions of the H^+ electrophile with the nucleophilic centers of the complexes are also supported by orbital interactions involving the Highest Occupied Molecular Orbitals (HOMOs) of the complexes shown in Scheme 2S. Both HOMOs correspond to Pt-P and Pd-P bonding molecular orbitals (MOs) localized mainly on the $Pt(\mu\text{-}P)_2Pd$ and $Pd(\mu\text{-}P)_2Pd$ "rhombus".

Scheme 2S

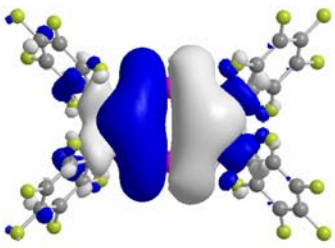

$[(C_6F_5)_2Pt(\mu\text{-}PH_2)_2Pd(C_6F_5)_2]^{2-}$

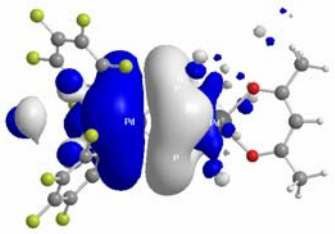

$[(C_6F_5)_2Pd(\mu\text{-}PH_2)_2Pd(acac)]^-$

Both the electrostatic and covalent interactions controlling the electrophilic attack of the nucleophilic centers of the complexes by the H^+ electrophile along with the weaker Pd-C_{ipso} than the Pt-C_{ipso} bond in the $[(C_6F_5)_2Pt(\mu\text{-}PH_2)_2Pd(C_6F_5)_2]^{2-}$ complex (compare also the respective bond lengths) accounts well for the observed selective breaking of the two Pd-C_{ipso}

bonds and the coordination of the Pd central atom with two solvent (CH_3CN) molecules affording the $[(C_6F_5)_2Pt(\mu\text{-}PH_2)_2Pd(NCCH_3)_2]$ complex.

Overall the solvation reactions of the $[(C_6F_5)_2Pt(\mu\text{-}PH_2)_2Pd(C_6F_5)_2]^{2-}$ and $[(C_6F_5)_2Pd(\mu\text{-}PH_2)_2Pd(acac)]^-$ complexes, under acidic conditions, yielding the $[(C_6F_5)_2Pt(\mu\text{-}PH_2)_2Pd(NCCH_3)_2]$ and $[(C_6F_5)_2Pd(\mu\text{-}PH_2)_2Pd(NCCH_3)_2]$ complexes, respectively are predicted to be strongly exothermic:

$$[(C_6F_5)_2Pt(\mu\text{-}PH_2)_2Pd(C_6F_5)_2]^{2-} \xrightarrow[-\,2C_6F_5H]{+\,2H^+ + 2NCCH_3} [(C_6F_5)_2Pt(\mu\text{-}PH_2)_2Pd(NCCH_3)_2] \quad \Delta_R H = 648\ kcal/mol$$

$$[(C_6F_5)_2Pd(\mu\text{-}PH_2)_2Pd(acac\text{-}O,O)]^- \xrightarrow[-\,acac\text{-}O,OH]{+\,2H^+ + 2NCCH_3} [(C_6F_5)_2Pd(\mu\text{-}PH_2)_2Pd(NCCH_3)_2] \quad \Delta_R H = 287\ kcal/mol$$

The higher exothermicity of the first reaction could be attributed to the two exothermic protonations taking place in the $[(C_6F_5)_2Pt(\mu\text{-}PH_2)_2Pd(C_6F_5)_2]^{2-}$ complex resulted in the formation of two strong C-H bonds, while in the second reaction only one protonation of the bidentate acac ligand of the $[(C_6F_5)_2Pd(\mu\text{-}PH_2)_2Pd(acac)]^-$ complex takes place forming only one O-H bond.

Equilibrium Geometry, Electronic Structure, and Bonding Mechanism in the $[(C_6F_5)_2M(\mu\text{-}PH_2)_2M'(NCCH_3)_2]$ (M = Pt, M′ = Pd; M = M′ = Pt or Pd) Complexes. The equilibrium geometries of the $[(C_6F_5)_2M(\mu\text{-}PH_2)_2M'(NCCH_3)_2]$ (M = M′ = Pt, **M1**; M = Pt, M′ = Pd; **M2**; M = M′ = Pd, **M3**) complexes are shown in Figure 4S, while the total electronic energies and some electronic properties of the complexes are given in Table 4S.

The salient structural feature of the $[(C_6F_5)_2M(\mu\text{-}PH_2)_2M'(NCCH_3)_2]$ (M = M′ = Pt, **M1**; M = Pt, M′ = Pd; **M2**; M = M′ = Pd, **M3**) complexes is the flexible dihedral angle between the two MP2 planes that describe the degree of folding of the $M(\mu\text{-}PH_2)_2M'$ ring along the P···P axis. The M-P-M′-P dihedral angles in **M1**, **M2** and **M3** were found to be 15.8, 28.0 and 34.4º, respectively. In all complexes both metal centers adopt distorted square planar coordination environments. The long intermetallic Pt···Pt, Pt···Pd and Pd···Pd distances of 3.736, 3.641 and 3.533 Å, respectively preclude any kind of intermetallic interactions. The absence of intermetallic interactions is also mirrored on the large Pt-P-Pt, Pt-P-Pd and Pd-P-Pd bond angles of 92.5, 96.8 and 100.2º, respectively. The folding along the P···P axis imposes a narrowing of the M-P-M′ bond angles and a shortening of the M···M′ separation distances. The coordinated MeCN ligands are slightly bent, the C≡N-M bond angles found in the range of 173.1-176.8º, with the bending being more pronounced in the dipalladium complex **M3**. The calculated Pt-NCMe and Pd-NCMe bond lengths of about 2.008 and 2.131 Å, respectively are indicative of the stronger interactions in the Pt than in the Pd complexes,

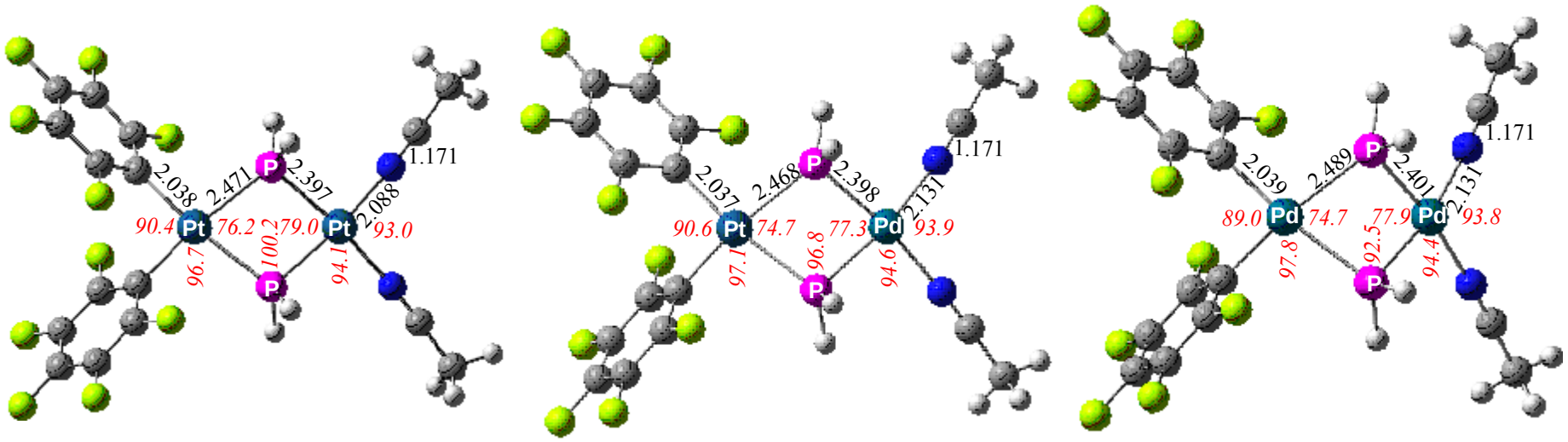

Figure 4S. Equilibrium geometries (bond lengths in Å, bond angles in deg) of the $[(C_6F_5)_2M(\mu\text{-}PH_2)_2M'(NCCH_3)_2]$ (M = M′ = Pt, **M1**; M = Pt, M′ = Pd; **M2**; M = M′ = Pd, **M3**) complexes computed at the B3LYP/lanl2dz level.

Table 4S. Total Electronic Energies and Selected Electronic Properties of the $[(C_6F_5)_2M(\mu\text{-}PH_2)_2M'(NCCH_3)_2]$ (M = M′ = Pt, **M1**; M = Pt, M′ = Pd; **M2**; M = M′ = Pd, **M3**) Complexes Computed at the B3LYP/lanl2dz Level of Theory

Property	**M1**	**M2**	**M3**
E (hartrees)	-1974.88070	-1982.44982	-1990.00699
ε_{HOMO} (eV)	-6.04	-6.14	-6.33
ε_{LUMO} (eV)	-2.09	-2.90	-2.68
η (eV)[a]	1.98	1.62	1.83
$q_{Pt(R)}$[b]	0.36 (0.38)[c]	0.36 (0.36)	
$q_{Pt(NCMe)}$	0.39 (-0.08)		
$q_{Pd(R)}$			0.44 (0.16)
$q_{Pd(NCMe)}$		0.42 (-0.10)	0.42 (-0.15)
$q_{C(Pt)}$	-0.34 (-0.29)	-0.34 (-0.32)	
$q_{C(Pd)}$			-0.31 (-0.10)
$q_{N(Pt)}$	-0.47 (0.005)		
$q_{N(Pd)}$		-0.47 (0.02)	-0.46 (0.03)
nec(Pt_R)[d]	$6s^{0.58}35d^{9.05}$	$6s^{0.58}5d^{9.05}$	
nec(Pt_{NCMe})	$6s^{0.60}5d^{8.99}$		
nec(Pd_R)			$5s^{0.40}4d^{9.16}$
nec(Pd_{NCMe})		$5s^{0.40}4d^{9.16}$	$5s^{0.39}4d^{9.17}$

[a] Hardness, $\eta = (\varepsilon_{LUMO} - \varepsilon_{HOMO})/2$. [b] Natural charges. [c] Figures in parentheses are the Mulliken net atomic charges. [d] Natural electron configuration

which is also reflected on the computed interaction energies of 171 and 166 kcal/mol, respectively. The computed harmonic vibrational frequencies (unscalled) due to the ν_{sym}(C≡N) and ν_{asym}(C≡N) vibrational modes of the two coordinated MeCN ligand were found at 2341 and 2347, 2339 and 2344 and 2339 and 2344 cm^{-1} in **M1**, **M2** and **M3**, respectively. The computed values are in excellent agreement to the experimental ones of 2286 and 2313 and 2290 and 2317 cm^{-1} for **2** and **3**, respectively.

The metal centers in **M1** acquire a positive natural atomic charge, which is slightly higher for the Pt center associated with the MeCN ligand. The opposite is true for the metal centers in **M3** where the Pd center associated with the MeCN ligand acquire a slightly lower positive natural atomic charge (Table 4S). In **M2** the Pd is the metal center acquiring the higher

positive natural atomic charge. The N donor atom of the MeCN ligands in all complexes acquires the higher negative natural atomic charge amounted to –0.47 |e|. According to the hardness values both homonuclear complexes are more stable than the heteronuclear one with the stability following the trend: **M1** > **M3** > **M2**.

The 3-D plots of the frontier molecular orbitals (FMOs) directly involved in the oxidative addition of I_2 to a representative complex **M2** are shown in Scheme 3S. Analogous are the 3-D plots of the FMOs of **M1** and **M3**. The HOMO of all complexes consists of an antibonding combination of nd_z^2 orbitals of the two metal centers mainly localized on the metal center coordinated with the C_6F_5 ligands, having also a small contribution from a π MO of the C_6F_5 ligands in an out-of-phase fashion. On the other hand, the LUMO consists of a bonding combination of $nd_{x^2-y^2}$ orbitals of the two metal centers mainly localized on the metal center coordinated with the MeCN ligands and having significant contribution from a σ* MO localized on the CN moiety participating in an antibonding combination mode.

Scheme 3S

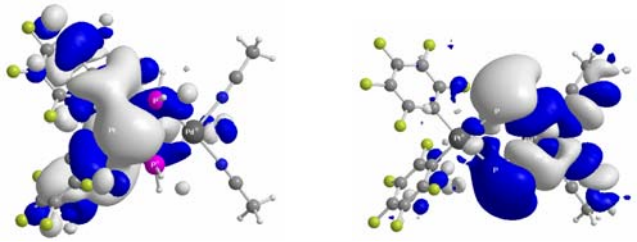

HOMO **LUMO**

M2

The nature of the FMOs of **M1**, **M2** and **M3** imply that the HOMO of the I_2 molecule, being a σ MO, could interact with the LUMO of the complexes which is mainly localized on the metal center coordinated with the MeCN ligands. The HOMO-LUMO interaction weakens both the I-I and M-NCMe bonds due to charge transfer from a bonding (HOMO of I_2) to an antibonding with respect to the M-NCMe bond MO. Moreover, possible interactions of the HOMOs of the complexes with the LUMO (a σ* MO) of I_2 molecule could not be excluded. Such interactions contribute further to the weakening of the I-I and M-NCMe bonds and the formation of the final oxidation product $[(C_6F_5)_2M(\mu\text{-}PH_2)_2M'I_2]$ (M = M′ = Pt, **M4**; M = Pt, M′ = Pd; **M5**; M = M′ = Pd, **M6**) products.

Equilibrium Geometry, Electronic Structure, and Bonding Mechanism in the $[(C_6F_5)_2M(\mu\text{-}PH_2)_2M'I_2]$ (M = Pt, M′ = Pd; M = M′ = Pt or Pd) Complexes. The equilibrium geometries of the $[(C_6F_5)_2M(\mu\text{-}PH_2)_2M'I_2]$ (M = M′ = Pt, M4; M = Pt, M′ = Pd;

M5; M = M′ = Pd, M6) complexes are shown in Figure 5S, while the total electronic energies and some electronic properties of the complexes are given in Table 5S.

Table 5S. Total Electronic Energies and Selected Electronic Properties of the $[(C_6F_5)_2M(\mu\text{-}PH_2)_2M'I_2]$ (M = M′ = Pt, **M4**; M = Pt, M′ = Pd; **M5**; M = M′ = Pd, **M6**) Complexes Computed at the B3LYP/lanl2dz Level of Theory

Property	**M4**	**M5**	**M6**
E (hartrees)	-1732.15597	-1739.74119	-1747.16640
ε_{HOMO} (eV)	-7.20	-7.24	-7.27
ε_{LUMO} (eV)	-5.23	-5.02	-5.01
η (eV)[a]	0.99	1.11	1.13
$q_{Pt(R)}$[b]	0.39 (0.31)[c]	0.37 (0.25)	
q_{PtI}	0.12 (-0.59)		
$q_{Pd(R)}$			0.41 (0.15)
q_{PdI}		0.24 (-0.21)	0.23 (-0.28)
$q_{C(Pt)}$	-0.38 (-0.36)	-0.40 (-0.39)	
$q_{C(Pd)}$			-0.30 (-0.24)
$q_{I(1)}$	-0.14 (0.09)	-0.09 (0.08)	-0.10 (0.06)
$q_{I(2)}$	-0.22 (0.05)	-0.27 (-0.04)	-0.27 (-0.04)
nec(Pt_R)[d]	$6s^{0.55}35d^{9.04}$	$6s^{0.55}5d^{9.06}$	
nec(Pt_I)	$6s^{0.64}5d^{9.20}$		
nec(Pd_R)			$5s^{0.38}4d^{9.20}$
nec(Pd_I)		$5s^{0.38}4d^{9.36}$	$5s^{0.39}4d^{9.36}$

[a] Hardness, $\eta = (\varepsilon_{LUMO} - \varepsilon_{HOMO})/2$. [b] Natural charges. [c] Figures in parentheses are the Mulliken net atomic charges. [d] Natural electron configuration.

The core structure of **M4**, **M5** and **M6** consists of a nearly planar $M(\mu\text{-}PH_2)_2M'$ "rhombus" with large P-M-P bond angles found in the range of 103.4-107.4º and small M-P-M′ bond angles found in the range of 72.5-76.4º. The short intermetallic Pt···Pt, Pt···Pd and Pd···Pd distances of 2.898, 2.936 and 2.922 Å, respectively strongly suggest the existence of intermetallic interactions consistent with the 30 valence electron count. Both metal centers being four-coordinated adopt a distorted square planar configuration. Overall, the B3LYP/lanl2dz calculations reproduce very well the experimentally observed structural parameters of **M4**. A characteristic structural feature of all complexes is the non-equivalence

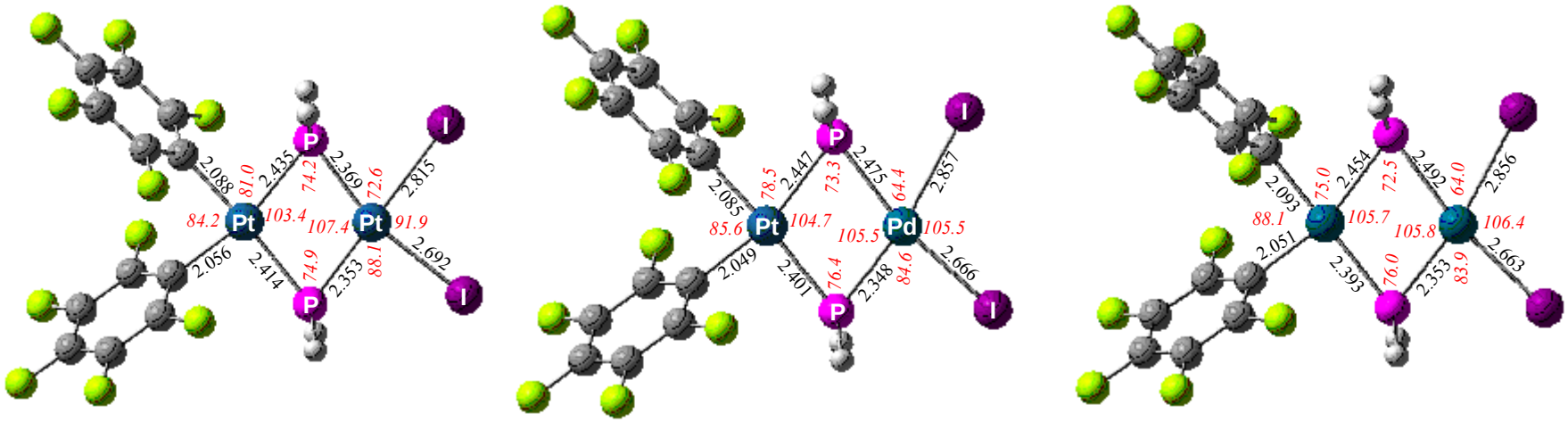

M4 **M5** **M6**

Figure 5S. Equilibrium geometries (bond lengths in Å, bond angles in deg) of the $[(C_6F_5)_2M(\mu\text{-}PH_2)_2M'I_2]$ (M = M′ = Pt, **M4**; M = Pt, M′ = Pd; **M5**; M = M′ = Pd, **M6**) complexes computed at the B3LYP/lanl2dz level.

of the M-I bonds, one of them being much shorter than the other (2.815 and 2.692 Å in M4; 2.857 and 2.666 Å in **M5**; 2.856 and 2.663 Å in **M6**). Moreover, there are some noticeable structural changes along the series of **M4**, **M5** and **M6** complexes. Thus, the I-M-I bond angle increases, while the P-M-I bond angle involving the longer M-I bond decreases as one goes from **M4** to **M6**. However, the most characteristic structural parameter of the complexes related with the reductive coupling of PH_2 and C_6F_5 is the narrowing of the P-Pt-C_{ipso} and P-Pd-C_{ipso} bond angles having the P atom common with the P-M-I bond angle involving the longer M-I bond. These angles were found to be 81.0, 78.5 and 75.0º for the **M4**, **M5** and **M6** complexes, respectively. The narrowing of the P-Pt-C_{ipso} and P-Pd-C_{ipso} bond angles forces the P donor atom of the bridging phosphido ligand to be closer to the C_{ipso} atom of the C_6F_5 ligand, the P-C_{ipso} separation distances being 2.949, 2.880 and 2.781 Å for **M4**, **M5** and **M6**, respectively. The P-C_{ipso} separation distances being shorter than the sum of the van der Waals radii of the P and C atoms (3.246 Å) indicate the existence of weak P···C_{ipso} interactions, which can promote the reductive coupling of PH_2 and C_6F_5. It is evident that the shorter P···C_{ipso} separation distance in the dipalladium complex **M6** corresponds to much stronger P···C_{ipso} interactions, which account well for our unsuccessful attempts to isolate the $[(C_6F_5)_2Pd(\mu\text{-}PPh_2)_2PdI_2]$ complex. Obviously, the $[(C_6F_5)_2Pd(\mu\text{-}PPh_2)_2PdI_2]$ complex immediately rearranges to the tetranuclear complex **10**, through the reductive coupling of PPh_2 and C_6F_5. It should be noted that according to the total electronic energies and the hardness values (Table 5S) the stability of the complexes follow the trend: **M6** > **M5** > **M4**, which means that the dipalladium complex is thermodynamically more stable, thereby one would expect **M6** to be isolated from the reaction mixture as is the case for **M4** and **M5**. However, it is the kinetic instability of **M6** towards the reductive coupling process responsible for **M6** to be a transient species that could not be isolated. Both metal centers in **M4**, **M5** and **M6** acquire a positive natural atomic charge, which is lower in the metal center coordinated with the iodide ligands. The iodide ligands acquire negative natural atomic charge, with that stronger coordinated with the metal center bearing much higher negative natural atomic charge (Table 5S). The two-electron (2e) reduction of **M4** and **M5** enforces the dissociation of one of the iodide ligands yielding **M7** and **M8**, respectively (Scheme 4S). The overall process is predicted to be exothermic, with exothermicities of 154 and 147 kcal/mol, respectively at the B3LYP/lanl2dz level.

Scheme 4S

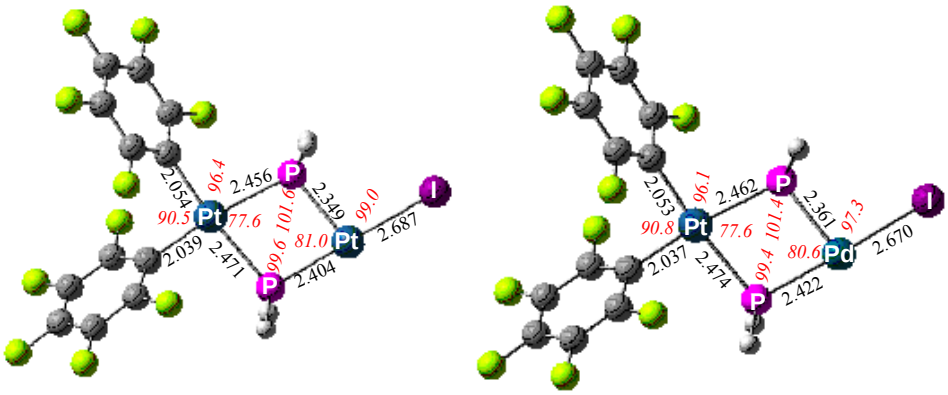

M7 **M8**

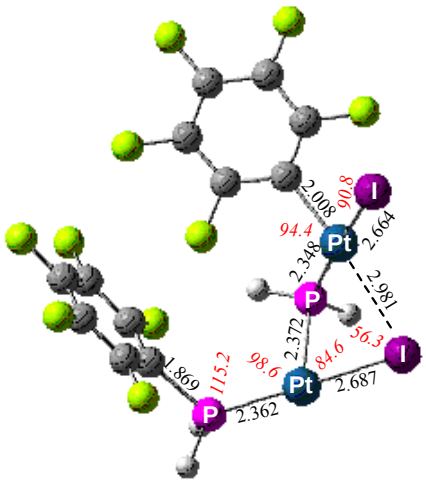

M9

To understand the dissociation of one of the iodide ligands upon 2e reduction of **M4** and **M5** we looked at the acceptor orbital (the LUMO) of the complexes. The 3-D plots of the HOMO and LUMO of a representative complex **M5** are shown in Scheme 5S. Analogous are the 3-D plots of the HOMO and LUMO of **M4** and **M6**.

Scheme 5S

HOMO **LUMO**

M5

It can be seen that the LUMOs of **M4**, **M5** and **M6** correspond to Pt-P and Pd-P bonding molecular orbitals localized mainly on the Pt(μ-P)$_2$Pt, Pt(μ-P)$_2$Pd and Pd(μ-P)$_2$Pd "rhombus", respectively with significant contribution from Pt-I and Pd-I antibonding

interactions related with the weaker Pt-I and Pd-I bonds. Therefore, the 2e reduction of the complexes accumulates electron density on the Pt-I or Pd-I antibonding LUMOs, thus enforcing the dissociation of the respective bonds and the formation of the monomeric species **M7** and **M8**. The nature of the FMOs of **M7** and **M8** (Scheme 6S) accounts well for their easy dimerization, which is supported by favorable HOMO-LUMO interactions.

Scheme 6S

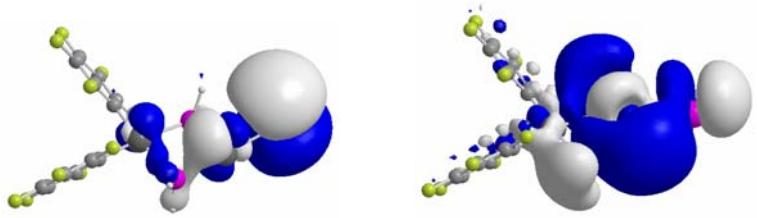

HOMO **LUMO**

M8

Thus, one molecule could act as a ligand through its donor orbital (HOMO) exhibiting high 5*p*(I) orbital character interacting with the acceptor orbital (LUMO) exhibiting high n*d*(M) character of the other molecule resulting in the formation of two M-I-M bridges. Along this line the formation of the dimeric species **6** and **7** can be easily understood.

Finally, the reductive coupling of PH_2 and C_6F_5 taking place immediately for **M6** and after stirring for a long period solutions of **M4** and **M5** (see experimental section) affords dinuclear species which dimerize directly to form the tetranuclear clusters. We optimized the geometry of the dinuclear species **M9** (Scheme 4) resulted from the reductive coupling of PH_2 and C_6F_5 in complex **M4** at the B3LYP/lanl2dz level. It can be seen that both Pt centers in **M9** are three-coordinated with a T-shaped coordination environment. The two coordination planes form a dihedral angle of 43.7º. However, the iodide ligand coordinated to the Pt center where the reductive coupling has occurred is also loosely associated with the other Pt center, thus forming a Pt-I···Pt bridge (the I···Pt separation distance is 2.981 Å). The long Pt···Pt distance of 3.464 Å excludes any kind of metal-metal interactions. Looking at the FMOs of **M9** shown in Scheme 7S it is easy to understand why these dinuclear species are directly dimerize to form the tetranuclear clusters.

Scheme 7S

HOMO **LUMO**

M9

The donor orbital (HOMO) of **M9** exhibits high 5*p*(I) orbital character of the terminal iodide ligand while the acceptor orbital (LUMO) exhibits high n*d*(M) character. Obviously, it is expected the favorable HOMO-LUMO interactions between two molecules to promote the dimerization and formation of the tetranuclear species. In general terms, the computed structural features of **M9** match well with those of the tetramnuclear species **8** determined experimentally.

Table S1
Cartesian Coordinates of Phosphido Platinum and/or Palladium Compounds
(B3LYP/LANL2DZ)

$[(C_6F_5)_2Pt(\mu\text{-}PH_2)_2Pd(C_6F_5)_2]^{2-}$ {Standard Orientation}

Pt	1.806674	-0.000511	-0.002372
Pd	-2.046972	-0.001373	-0.002478
P	-0.119322	1.527792	-0.222307
P	-0.118688	-1.531417	0.204815
F	2.629158	2.504186	1.940254
F	4.545009	4.443585	1.690927
F	6.216017	4.510549	-0.536895
F	5.941182	2.577682	-2.527706
F	4.045675	0.612435	-2.308117
F	4.037188	-0.611954	2.311885
F	5.933193	-2.576236	2.538725
F	6.216996	-4.508476	0.548545
F	4.554824	-4.441849	-1.685956
F	2.638854	-2.503716	-1.942408
C	3.242520	1.461663	-0.172712
C	3.431989	2.466133	0.795633
C	4.400635	3.473928	0.695816
C	5.245536	3.514132	-0.418334
C	5.101123	2.540889	-1.411508
C	4.118478	1.551186	-1.269916
C	3.243101	-1.461420	0.173417
C	4.114755	-1.550652	1.274034
C	5.097548	-2.539672	1.419206
C	5.246469	-3.512546	0.426313
C	4.405964	-3.472565	-0.691169
C	3.437102	-2.465317	-0.794571
F	-3.036156	2.276322	2.098476
F	-4.972438	4.219278	1.919744
F	-6.490865	4.489591	-0.397934
F	-6.054397	2.774514	-2.550219
F	-4.137299	0.808463	-2.396263
F	-4.142153	-0.798653	2.391145
F	-6.062429	-2.761138	2.550376
F	-6.497242	-4.485367	0.405081
F	-4.974436	-4.227413	-1.911041
F	-3.035119	-2.288306	-2.095117
C	-3.503641	1.457991	-0.141761
C	-3.768217	2.350315	0.907739
C	-4.745034	3.354570	0.846648
C	-5.513419	3.496717	-0.314368
C	-5.288242	2.631496	-1.390223
C	-4.299923	1.642501	-1.280094
C	-3.504621	-1.459661	0.141093
C	-4.303634	-1.637656	1.278603
C	-5.293685	-2.624617	1.391311
C	-5.517939	-3.494515	0.319059
C	-4.747288	-3.358616	-0.841169
C	-3.768660	-2.356263	-0.904889
H	-0.100270	2.255111	-1.464563
H	-0.088116	2.646091	0.678726
H	-0.099180	-2.275335	1.437150
H	-0.087690	-2.638072	-0.710377

$[(C_6F_5)Pt(\mu\text{-}PH_2)_2Pd(C_6F_5)_2]^-$ {Standard Orientation}

Pt	-2.326760	-1.229378	-0.266131
Pd	1.201093	-0.174745	-0.061175
P	-1.091956	0.746804	0.069437
P	-0.108638	-2.233687	-0.526245
F	-3.994798	0.863554	-2.155713
F	-6.499092	1.946459	-1.855750
F	-8.016669	1.385676	0.408644
F	-6.991815	-0.286626	2.383938
F	-4.491490	-1.392450	2.109875
C	-4.141290	-0.314376	-0.036692
C	-4.708979	0.543033	-0.996449
C	-5.983260	1.112934	-0.870936
C	-6.751060	0.834940	0.265698
C	-6.230867	-0.007677	1.255054
C	-4.952272	-0.555137	1.087731
F	1.193110	2.595454	-1.687526
F	2.520356	4.973387	-1.295545
F	4.200762	5.301259	0.900921
F	4.543504	3.210527	2.706728
F	3.242272	0.820490	2.331336
F	3.577494	0.024061	-2.258819
F	5.995431	-1.275902	-2.424075
F	6.740695	-3.116765	-0.470583
F	5.024860	-3.648936	1.656159
F	2.597295	-2.371113	1.838691
C	2.183175	1.609692	0.295262
C	2.040800	2.697423	-0.575357
C	2.695950	3.923741	-0.399759
C	3.541196	4.094594	0.702595
C	3.709890	3.039531	1.606188
C	3.031876	1.831459	1.386670
C	3.002147	-1.119052	-0.198570
C	3.898976	-0.889910	-1.249031
C	5.138455	-1.536440	-1.359535
C	5.518003	-2.462078	-0.381615
C	4.651026	-2.725223	0.685431
C	3.422120	-2.055398	0.755270
H	-1.645243	1.322943	1.264913
H	-1.626396	1.673458	-0.886310
H	0.152316	-2.816394	-1.809561
H	0.192703	-3.340983	0.329114H

$[(C_6F_5)_2Pt(\mu\text{-}PH_2)_2Pd(C_6F_5)]^-$ {Standard Orientation}

Pt	-0.926266	-0.251680	-0.048956
Pd	2.562606	-1.497755	-0.190664
P	1.395937	0.538656	0.048470
P	0.280262	-2.395002	-0.381228
F	-0.699123	2.489051	-1.776011
F	-1.883811	4.941744	-1.474966
F	-3.596971	5.431848	0.666994
F	-4.112117	3.409298	2.511961
F	-2.954823	0.942554	2.232169
F	-3.293742	0.032215	-2.244225
F	-5.759754	-1.152075	-2.407286
F	-6.607119	-2.931558	-0.436391
F	-4.930161	-3.511425	1.710403
F	-2.455957	-2.353109	1.897277
C	-1.787394	1.602927	0.206572
C	-1.560642	2.664172	-0.685508
C	-2.145717	3.930221	-0.556204
C	-3.007146	4.182600	0.516667
C	-3.262033	3.162341	1.438626
C	-2.654100	1.910664	1.268602
C	-2.769200	-1.107783	-0.164915

C	-3.656810	-0.852098	-1.223823
C	-4.924288	-1.440525	-1.332817
C	-5.355289	-2.333993	-0.347448
C	-4.507397	-2.621970	0.727494
C	-3.248278	-2.012672	0.798448
F	4.487865	-0.133049	-2.409104
F	7.012667	0.950446	-2.197735
F	8.260765	1.124839	0.281830
F	6.960240	0.202298	2.561325
F	4.435284	-0.886025	2.375789
C	4.375601	-0.555917	-0.024924
C	5.072830	-0.068831	-1.139199
C	6.356533	0.489650	-1.063577
C	6.989266	0.579885	0.182199
C	6.330353	0.113615	1.326497
C	5.047455	-0.437087	1.199416
H	1.938597	1.153782	1.226047
H	1.939900	1.413701	-0.947112
H	-0.058945	-3.025783	-1.623677
H	-0.125296	-3.413379	0.540306

[$(C_6F_5)_2Pd(\mu\text{-}PH_2)_2Pd(acac)]^-$ {Standard Orientation}

F	3.577901	-4.280471	-1.648537
F	4.889069	-4.380059	0.806033
C	3.253742	-3.356688	-0.657613
C	3.916783	-3.412313	0.573871
F	1.643963	-2.383473	-2.117106
C	2.276219	-2.374658	-0.867937
F	4.242344	-2.543307	2.797814
C	3.587345	-2.486683	1.569764
C	2.601748	-1.522520	1.312368
C	1.912756	-1.425779	0.097120
F	3.032087	0.710119	-2.167198
F	2.321383	-0.627719	2.352763
P	-1.461937	-1.602166	-0.312530
F	4.868503	2.748739	-1.984278
Pd	0.455142	-0.031547	-0.277485
C	2.899520	1.613096	-1.104546
C	-6.814096	-2.504360	0.878925
O	-4.731198	-1.515529	0.290663
C	3.851877	2.640498	-1.038063
C	1.858191	1.462539	-0.180752
C	-5.993802	-1.276411	0.506134
Pd	-3.296525	-0.072466	-0.234682
C	3.777157	3.577625	-0.001866
P	-1.500624	1.417371	-0.750771
C	1.823562	2.425905	0.836338
F	4.709244	4.607007	0.084565
C	2.751461	3.470563	0.944572
F	0.817025	2.382967	1.808333
C	-6.637190	-0.015587	0.425161
O	-4.776144	1.417427	-0.193048
F	2.673850	4.405449	1.974131
C	-6.031406	1.223670	0.097185
C	-6.887155	2.483198	0.068803
H	-1.642855	-2.443382	-1.461886
H	-1.649660	-2.576693	0.724762
H	-6.745379	-3.245325	0.072289
H	-7.866300	-2.261495	1.058275
H	-6.389191	-2.964601	1.779923
H	-1.688287	1.856756	-2.105944
H	-1.729487	2.656587	-0.065570
H	-7.700032	0.003519	0.640558
H	-7.936111	2.277711	0.304774
H	-6.488783	3.207860	0.790320
H	-6.821755	2.944573	-0.924662

[$(C_6F_5)_2Pt(\mu\text{-}PH_2)_2Pt(NCMe)_2$], M1 {Standard Orientation}

F	3.370152	-4.493073	-1.438795
C	-6.199376	-3.513023	1.078391
F	1.457290	-2.599166	-1.952408
C	-5.325012	-2.404250	0.694164
C	3.157255	-3.466642	-0.528320
P	-1.412799	-1.588618	-0.374594
F	4.873026	-4.384831	0.905176
C	2.190812	-2.481738	-0.766536
N	-4.611496	-1.528197	0.388036
C	3.914767	-3.417091	0.647032
Pt	-3.236232	-0.050137	-0.141148
C	1.927613	-1.421709	0.116318
Pt	0.496861	-0.024095	-0.276455
F	3.181300	0.561440	-2.023721
C	3.686365	-2.383847	1.561831
P	-1.446651	1.440863	-0.705827
N	-4.637730	1.482868	0.072582
C	2.709441	-1.417808	1.283151
F	4.425059	-2.333179	2.735710
C	-5.358204	2.396072	0.203671
C	2.996913	1.533573	-1.037985
F	2.527557	-0.421507	2.245378
C	1.893708	1.456317	-0.172691
C	-6.240713	3.552272	0.363994
F	5.020592	2.587496	-1.866127
C	3.952716	2.557508	-0.980576
C	1.808471	2.492698	0.770455
F	0.742427	2.523209	1.677747
C	3.824484	3.566684	-0.020200
C	2.739860	3.533800	0.863258
F	4.755957	4.590782	0.051503
F	2.600311	4.534036	1.816760
H	-6.091591	-4.341175	0.368993
H	-5.934978	-3.872255	2.079317
H	-7.246228	-3.190208	1.085260
H	-1.671183	-2.336217	-1.569925
H	-1.609293	-2.618931	0.604010
H	-1.725442	1.872909	-2.045556
H	-1.669158	2.667663	-0.000726
H	-7.071115	3.308949	1.035857
H	-5.682161	4.394482	0.787693
H	-6.649268	3.854783	-0.606687

[$(C_6F_5)_2Pt(\mu\text{-}PH_2)_2Pt(NCMe)$] {Standard Orientation}

F	-1.833371	4.933580	-1.374756
C	7.444825	1.671382	0.540647
F	-0.239211	2.723385	-1.644595
C	6.192178	0.938382	0.358573
C	-2.022018	3.847424	-0.532949
P	1.965528	1.092968	-0.040398
F	-3.802552	5.024290	0.596880
C	-1.230802	2.698884	-0.651888
N	5.190293	0.348155	0.211979
C	-3.010060	3.898233	0.456158
Pt	3.464907	-0.755068	-0.054433
C	-1.367332	1.566666	0.166370
Pt	-0.184578	-0.086031	-0.081076
F	-2.662103	-0.172763	-2.169885
C	-3.178478	2.801219	1.307936
P	1.432373	-1.955031	-0.345899
C	-2.363697	1.670985	1.151728
F	-4.144948	2.848375	2.300039
C	-2.805083	-1.143393	-1.176821
F	-2.577386	0.623716	2.048509
C	-1.837101	-1.263792	-0.168366
F	-4.862311	-1.807307	-2.275422
C	-3.938169	-1.965117	-1.254285

C	-2.075475	-2.275926	0.774178
F	-1.165878	-2.482414	1.815355
C	-4.135541	-2.959190	-0.290014
C	-3.193845	-3.116459	0.733632
F	-5.246534	-3.783081	-0.350513
F	-3.379270	-4.101434	1.691924
H	7.502816	2.503697	-0.169699
H	7.505341	2.071461	1.558930
H	8.299020	1.005935	0.372486
H	2.470326	1.864581	-1.138223
H	2.476985	1.868460	1.055692
H	1.512434	-2.639108	-1.601078
H	1.412509	-3.048341	0.575013

$[(C_6F_5)_2Pt(\mu\text{-}PH_2)_2Pd(NCMe)_2]$, M2 {Standard Orientation}

F	3.349234	-4.444852	-1.190958
C	-6.139792	-3.596101	1.529881
F	1.476214	-2.616166	-2.003995
C	-5.344676	-2.505147	0.963536
C	2.977348	-3.415349	-0.337102
P	-1.639545	-1.658087	-0.827194
F	4.493465	-4.264728	1.342740
C	2.027735	-2.463335	-0.727682
N	-4.696026	-1.641841	0.509513
C	3.555393	-3.329556	0.934403
Pd	-3.419908	-0.138368	-0.301552
C	1.611992	-1.400985	0.091846
Pt	0.213117	-0.055683	-0.522881
F	3.159984	0.579900	-1.772291
C	3.167365	-2.294407	1.791358
P	-1.729869	1.315124	-1.183619
N	-4.735915	1.457926	0.209340
C	2.214509	-1.361261	1.359837
F	3.726113	-2.209134	3.059143
C	-5.363929	2.392246	0.533022
C	2.764222	1.570981	-0.872029
F	1.865316	-0.360727	2.270946
C	1.522565	1.475924	-0.222765
C	-6.125140	3.574466	0.940072
F	4.872573	2.675580	-1.346093
C	3.659486	2.631743	-0.674484
C	1.230661	2.536968	0.649413
F	0.011286	2.557222	1.341455
C	3.322951	3.663073	0.208777
C	2.093874	3.615230	0.875700
F	4.191921	4.722738	0.416152
F	1.745963	4.636871	1.750516
H	-6.449309	-4.288249	0.739009
H	-5.547840	-4.148769	2.267879
H	-7.034895	-3.200804	2.022250
H	-1.930145	-2.184071	-2.128511
H	-1.831209	-2.834626	-0.030102
H	-2.060012	1.454458	-2.572350
H	-2.005850	2.641052	-0.719516
h	-7.029323	3.279233	1.483362
H	-5.512688	4.206375	1.592972
H	-6.417250	4.158172	0.060156

$[(C_6F_5)_2Pd(\mu\text{-}PH_2)_2Pd(NCMe)_2]$, M3 {Standard Orientation}

F	3.849445	-4.093888	-1.209197
C	-5.688620	-3.635615	1.848818
F	1.994422	-2.316421	-2.200359
C	-4.993371	-2.571573	1.122480
C	3.224063	-3.196851	-0.354694
P	-1.567740	-1.755006	-1.171476
F	4.461070	-4.117505	1.506124

C	2.281325	-2.277292	-0.833496
N	-4.424264	-1.727944	0.542400
C	3.534948	-3.213043	1.010693
Pd	-3.287807	-0.233341	-0.468070
C	1.623240	-1.357659	-0.008137
Pd	0.229127	-0.083472	-0.765326
F	3.234514	0.759249	-1.763731
C	2.894759	-2.314775	1.871997
P	-1.730063	1.235616	-1.553068
N	-4.525846	1.363866	0.204203
C	1.957907	-1.411858	1.349110
F	3.190284	-2.336009	3.228478
C	-5.087887	2.302442	0.622759
C	2.723005	1.673517	-0.840746
F	1.340996	-0.545367	2.257800
C	1.451284	1.477295	-0.288891
C	-5.761917	3.490994	1.147692
F	4.791456	2.921851	-1.092601
C	3.538659	2.767838	-0.517329
C	1.031627	2.457837	0.617453
F	-0.236955	2.366294	1.210816
C	3.077935	3.722521	0.396857
C	1.809834	3.567838	0.968918
F	3.865460	4.813829	0.727594
F	1.341136	4.516115	1.869834
H	-5.841636	-4.501812	1.195678
H	-5.094940	-3.949611	2.714561
H	-6.664432	-3.283365	2.200487
H	-1.939582	-2.170939	-2.493430
H	-1.787980	-2.981785	-0.460811
H	-2.135741	1.228176	-2.929668
H	-2.105080	2.571145	-1.193387
H	-6.549196	3.204414	1.853331
H	-5.038915	4.129441	1.667708
H	-6.212627	4.064088	0.329962

[$(C_6F_5)_2Pd(\mu\text{-}PH_2)_2Pd(NCMe)$] {Standard Orientation}

F	-1.809615	4.750121	-1.556049
C	7.683031	1.217228	1.309877
F	-0.378446	2.459957	-2.086013
C	6.470866	0.546066	0.838463
C	-1.762338	3.732757	-0.614679
P	2.362252	0.917742	-0.604192
F	-3.141352	5.044268	0.871757
C	-1.048008	2.552918	-0.859708
N	5.497793	0.010073	0.462920
C	-2.432532	3.885280	0.605216
Pd	3.736839	-0.993963	-0.176144
C	-0.966354	1.499957	0.059024
Pd	0.120079	-0.168026	-0.381591
F	-2.645770	-0.190887	-2.084075
C	-2.370547	2.860486	1.556754
P	1.699091	-2.059437	-0.824917
C	-1.643116	1.696579	1.268492
F	-3.022961	3.012951	2.770540
C	-2.675212	-1.128548	-1.050196
F	-1.609006	0.713125	2.259320
C	-1.578374	-1.259147	-0.191495
F	-4.896693	-1.749209	-1.805292
C	-3.833429	-1.910075	-0.930575
C	-1.696500	-2.231059	0.808162
F	-0.640292	-2.442889	1.701086
C	-3.912774	-2.869199	0.085951
C	-2.833602	-3.034005	0.962986
F	-5.045938	-3.653442	0.219472
F	-2.903890	-3.988323	1.966777
H	7.840903	2.147082	0.752376
H	7.592468	1.455897	2.375284

H	8.554425	0.568900	1.166495
H	2.918639	1.323785	-1.865041
H	3.000817	1.884165	0.247479
H	1.983611	-2.541006	-2.146445
H	1.725239	-3.288891	-0.085449

$[(C_6F_5)_2Pt(\mu\text{-}PH_2)_2PtI_2]$, M4 {Standard Orientation}

Pt	-0.694934	-0.146551	-0.034949
Pt	2.202919	-0.157221	-0.024374
I	3.883313	2.070287	0.336592
I	4.306148	-1.814409	-0.288147
P	0.813766	1.720487	0.365070
P	0.798229	-2.019260	-0.326115
F	-1.493580	2.259123	-2.056952
F	-3.544005	4.096912	-1.986634
F	-5.212708	4.247883	0.234427
F	-4.810348	2.531722	2.386444
F	-2.783050	0.671877	2.317174
F	-3.059416	-0.461212	-2.248458
F	-5.298776	-2.054060	-2.269004
F	-5.783802	-3.822345	-0.176863
F	-3.981889	-3.991099	1.937285
F	-1.723205	-2.417000	1.961885
C	-2.104769	1.385245	0.110190
C	-2.329623	2.284114	-0.941492
C	-3.357457	3.235688	-0.922906
C	-4.196889	3.315754	0.194771
C	-3.991327	2.450230	1.276797
C	-2.953648	1.509702	1.218969
C	-2.342648	-1.370468	-0.125148
C	-3.265692	-1.326349	-1.178623
C	-4.413264	-2.130968	-1.211044
C	-4.659997	-3.022191	-0.160091
C	-3.753570	-3.102127	0.904474
C	-2.618022	-2.282471	0.902427
H	0.723364	2.813009	-0.539303
H	0.742858	2.304698	1.659559
H	0.910702	-3.061900	0.634838
H	0.917314	-2.674682	-1.583466

$[(C_6F_5)_2Pt(\mu\text{-}PH_2)_2PdI_2]$, M5 {Standard Orientation}

Pt	-0.485050	-0.174938	-0.041662
I	3.775268	2.296236	0.416797
I	4.396597	-1.985245	-0.356094
P	0.971259	1.747785	0.367656
P	1.014820	-2.028370	-0.316238
F	-1.335274	2.099208	-2.181661
F	-3.388479	3.938342	-2.171567
F	-4.981211	4.242030	0.088302
F	-4.504630	2.681855	2.340023
F	-2.473757	0.820546	2.332423
F	-2.860860	-0.574566	-2.225112
F	-5.090979	-2.179381	-2.171632
F	-5.544548	-3.883418	-0.019345
F	-3.720081	-3.974362	2.080246
F	-1.471080	-2.388213	2.033003
C	-1.868827	1.380382	0.061194
C	-2.132324	2.204249	-1.043700
C	-3.161893	3.153716	-1.057395
C	-3.964497	3.310129	0.079732
C	-3.721548	2.522614	1.212758
C	-2.683251	1.581962	1.185518
C	-2.115887	-1.413058	-0.082316

C	-3.050393	-1.407443	-1.126727
C	-4.193627	-2.218814	-1.121358
C	-4.424612	-3.077523	-0.040277
C	-3.506784	-3.118381	1.016582
C	-2.375659	-2.293540	0.977039
H	0.724465	2.854359	-0.492454
H	0.773082	2.289580	1.668502
H	1.133043	-3.074641	0.641553
H	1.113389	-2.705504	-1.564663
H	2.450518	-0.190793	-0.050005

[$(C_6F_5)_2Pt(\mu\text{-}PH_2)_2PdI$], M7 {Standard Orientation}

Pt	-0.336158	-0.176934	-0.139599
Pd	3.303423	-1.008455	-0.132388
I	5.604614	0.288342	0.255884
P	1.887446	0.880641	-0.124416
P	1.173427	-2.108745	-0.474436
F	-0.496108	2.548196	-1.883634
F	-1.945024	4.849094	-1.545482
F	-3.625112	5.152859	0.656639
F	-3.836973	3.095912	2.523461
F	-2.415191	0.777660	2.207249
F	-2.850429	-0.227061	-2.206223
F	-5.130589	-1.747893	-2.231893
F	-5.608647	-3.614297	-0.218392
F	-3.751478	-3.936399	1.832930
F	-1.456957	-2.437278	1.880746
C	-1.404186	1.553943	0.138501
C	-1.333028	2.629224	-0.763590
C	-2.055178	3.820251	-0.615238
C	-2.900933	3.978779	0.487584
C	-3.003290	2.941773	1.420311
C	-2.262534	1.766800	1.230668
C	-2.056298	-1.267669	-0.160448
C	-3.028444	-1.145754	-1.166990
C	-4.204584	-1.907561	-1.205497
C	-4.450333	-2.845960	-0.198392
C	-3.512670	-3.003933	0.828065
C	-2.350550	-2.222525	0.828352
H	2.329711	1.668773	-1.234506
H	2.332704	1.705111	0.958718
H	1.099186	-2.724669	-1.768428
H	0.964404	-3.251296	0.365204

[$(C_6F_5)_2Pd(\mu\text{-}PH_2)_2PdI_2$], M6 {Standard Orientation}

Pd	-0.519340	-0.203249	-0.088976
I	3.696910	2.302699	0.406520
I	4.338016	-2.006407	-0.334724
P	0.902938	1.759751	0.285335
P	0.979381	-2.049371	-0.348696
F	-1.450130	2.010377	-2.253180
F	-3.561696	3.797338	-2.228113
F	-5.031545	4.177961	0.099492
F	-4.389108	2.760903	2.400950
F	-2.296394	0.955270	2.376145
F	-2.901883	-0.671878	-2.253098
F	-5.147457	-2.267001	-2.121167
F	-5.579230	-3.897433	0.090253
F	-3.731465	-3.931284	2.170454
F	-1.469767	-2.351333	2.042588
C	-1.845858	1.408936	0.049112
C	-2.191715	2.159986	-1.082753
C	-3.248124	3.079682	-1.090510
C	-3.990091	3.274853	0.082654
C	-3.662581	2.558978	1.243209
c	-2.598627	1.648315	1.206295

C	-2.144863	-1.452604	-0.095422
C	-3.085763	-1.473607	-1.128967
C	-4.234159	-2.277249	-1.083485
C	-4.454611	-3.099239	0.029061
C	-3.524792	-3.111495	1.076885
C	-2.389808	-2.293707	0.994318
Pd	2.402328	-0.198828	-0.061608
H	0.684305	2.829955	-0.626656
H	0.663339	2.358877	1.553749
H	1.097115	-3.094356	0.611598
H	1.105975	-2.741486	-1.587902

$[(C_6F_5)_2Pt(\mu\text{-}PH_2)(\mu\text{-}I)Pt(PPh_2C_6F_5)(C_6F_5)]^-$, M9 {Standard Orientation}

Pt	0.425260	-2.643707	-0.422851
Pt	1.429154	0.666716	-0.236083
I	2.956153	-1.877088	0.051297
I	2.739982	1.979438	1.675481
P	-1.837741	-3.300559	-0.582349
P	0.331363	-0.708400	-1.790468
F	-2.666630	-2.708044	2.296093
F	-4.400419	-0.763637	3.240301
F	-5.706332	0.910407	1.451629
F	-5.268769	0.638445	-1.281997
F	-3.525299	-1.294073	-2.213908
F	-1.636323	0.890793	0.579783
F	-3.403498	2.956404	0.394390
F	-2.626602	5.392987	-0.746466
F	-0.038054	5.684710	-1.720427
F	1.753130	3.615509	-1.563641
C	-3.076959	-2.042199	0.027936
C	-3.314212	-1.872605	1.398814
C	-4.185920	-0.894875	1.888710
C	-4.844509	-0.048275	0.986788
C	-4.627510	-0.188502	-0.389935
C	-3.748698	-1.176293	-0.844197
C	0.143329	2.194768	-0.445172
C	-1.179011	2.092387	0.011491
C	-2.109159	3.134124	-0.075115
C	-1.725850	4.349736	-0.648716
C	-0.420166	4.491041	-1.135741
C	0.484087	3.423946	-1.037290
H	-2.384198	-3.645286	-1.852764
H	-2.179525	-4.446748	0.196202
H	-1.025078	-0.530055	-2.214917
H	0.941651	-1.153753	-3.005862

C_6F_5H {Standard Orientation}

F	-2.403926	-1.657681	0.000049
F	-2.408358	1.117606	-0.000046
F	-0.000093	2.501499	-0.000005
F	2.408421	1.117564	0.000052
F	2.403916	-1.657633	-0.000032
C	0.000007	-1.693696	-0.000037
C	-1.198698	-0.975516	0.000011
C	-1.215208	0.425856	0.000011
C	0.000019	1.123859	0.000007
C	1.215279	0.425931	-0.000012
C	1.198647	-0.975468	-0.000017
H	0.000081	-2.777991	0.000056

$C_6F_5^-$ {Standard Orientation}

F	0.000000	2.449645	-1.675235
F	0.000000	2.417692	1.107660
F	0.000000	0.000000	2.480162

F	0.000000	-2.417692	1.107660
F	0.000000	-2.449645	-1.675235
C	0.000000	0.000000	-1.781368
C	0.000000	1.163872	-1.029885
C	0.000000	1.212650	0.372573
C	0.000000	0.000000	1.078476
C	0.000000	-1.212650	0.372573
C	0.000000	-1.163872	-1.029885

***acac*H {Standard Orientation}**

C	-2.579949	-0.747951	0.000258
O	-1.242510	1.264175	-0.000110
C	-1.249195	-0.026592	-0.000522
C	-0.006680	-0.768603	-0.000343
O	1.266260	1.255393	0.000190
C	1.211244	-0.099602	-0.000126
C	2.556611	-0.764290	0.000155
H	-3.154506	-0.451081	0.886553
H	-2.464781	-1.835890	-0.006374
H	-3.161394	-0.440444	-0.877762
H	-0.022767	-1.850669	-0.000465
H	0.301349	1.616487	0.000317
H	2.465202	-1.853731	0.000298
H	3.127394	-0.449618	-0.882569
H	3.127325	-0.449367	0.882824

MeCN {Standard Orientation}

N	1.457525	0.000941	-0.000001
C	0.277116	-0.002232	0.000027
C	-1.191612	0.000457	0.000012
H	-1.573065	-0.555964	-0.863390
H	-1.573188	-0.467668	0.914218
H	-1.569445	1.027697	-0.051049

Table S2

Energetic Results

Compound	Sum of electronic and zero-point Energies (a.u.)	Sum of electronic and thermal Energies (a.u.)	Sum of electronic and thermal Enthalpies (a.u.)	Sum of electronic and thermal Free Energies (a.u.)
$[(C_6F_5)_2Pt(\mu\text{-}PH_2)_2Pd(C_6F_5)_2]^{2-}$	-3172.705070			
$[(C_6F_5)Pt(\mu\text{-}PH_2)_2Pd(C_6F_5)_2]^{-}$	-2444.668983	-2444.630369	-2444.629425	-2444.746974
$[(C_6F_5)_2Pt(\mu\text{-}PH_2)_2Pd(C_6F_5)]^{-}$	-2444.681323	-2444.643705	-2444.642761	-2444.756224
$[(C_6F_5)_2Pd(\mu\text{-}PH_2)_2Pd(acac)]^{-}$	-2069.574940	-2069.537841	-2069.536897	-2069.648866
$[(C_6F_5)_2Pt(\mu\text{-}PH_2)_2Pt(NCMe)_2]$, M1	-1974.652380	-1974.615582	-1974.614638	-1974.730147
$[(C_6F_5)_2Pt(\mu\text{-}PH_2)_2Pt(NCMe)]$	-1841.925743	-1841.893005	-1841.892060	-1841.997124
$[(C_6F_5)_2Pt(\mu\text{-}PH_2)_2Pd(NCMe)_2]$, M2	-1982.222063	-1982.184024	-1982.183080	--1982.301238
$[(C_6F_5)_2Pd(\mu\text{-}PH_2)_2Pd(NCMe)_2]$, M3	-1989.779822	-1989.741662	-1989.740718	-1989.857986
$[(C_6F_5)_2Pd(\mu\text{-}PH_2)_2Pd(NCMe)]$	-1857.059864	-1857.026485	-1857.025541	-1857.131599
$[(C_6F_5)_2Pt(\mu\text{-}PH_2)_2PtI_2]$, M4	-1732.020531	-1731.988135	-1731.987191	-1732.092568
$[(C_6F_5)_2Pd(\mu\text{-}PH_2)_2PdI]$, M7	-1720.793057	-1720.762894	-1720.761950	-1720.861337
$[(C_6F_5)_2Pt(\mu\text{-}PH_2)_2PdI_2]$, M5	-1739.606028	-1739.573564	-1739.572619	-1739.677706
$[(C_6F_5)_2Pt(\mu\text{-}PH_2)_2PdI]$, M8	-1728.370741	-1728.340436	-1728.339492	-1728.438467
$[(C_6F_5)_2Pd(\mu\text{-}PH_2)_2PdI_2]$, M6	-1747.166403	-1747.133762	-1747.132818	-1747.237902
M9	-1732.032963	-1732.000961	-1732.000017	-1732.104273
C_6F_5H	-728.329190	-728.320391	-728.319446	-728.363315
$C_6F_5^-$	-727.766558	-727.757580	-727.756636	-727.800392
***acac*H**	-345.635277	-345.628281	-345.627336	-345.666420
MeCN	-132.682735	-132.679142	-132.678198	-132.706770